Int. J. Heat Mass Transfer. Vol. 1, pp. 325–335. Pergamon Press 1961. Printed in Great Britain.

AN ANALYSIS OF LAMINAR FILM BOILING WITH VARIABLE PROPERTIES

P. W. McFADDEN* and R. J. GROSH†
Purdue University, Lafayette, Indiana, U.S.A.

(*Received* 16 *July* 1959)

Abstract—An analysis is made of stable, laminar, free convection, film boiling from isothermal vertical plates and horizontal cylinders surrounded by a saturated liquid. The mathematical techniques of boundary-layer theory are used and the boundary-layer equations are reduced to ordinary differential equations by means of a transformation similar to that used in free convection and condensation. The equations are solved for compressible flow with variable specific heat. Numerical results are presented for near critical water at 2800 and 3100 Lb/in² with wall-to-liquid temperature differences of 250, 500 and 1000°F. Results for heat transfer, velocity distribution and temperature distribution are included and compared to solutions obtained by assuming constant properties.

Résumé—Une analyse est faite du film laminaire, de convection libre en régime stable et à l'ébullition sur des plaques isothermes verticales et des cylindres horizontaux recouverts d'un liquide saturé. Les techniques mathématiques de la théorie de la couche limite sont utilisées et les équations de la couche limite sont réduites à des équations différentielles ordinaires grâce à une transformation analogue à celle utilisée pour la convection libre et la condensation. Les équations sont résolues pour un écoulement compressible avec chaleur spécifique variable. Des résultats numériques sont présentés pour l'eau au voisinage du point critique à 2800 et 3100 lb/in² avec des différences de température entre paroi et liquide de 250, 500, 1000°F. Des résultats sur le transfert de chaleur, la distribuiton des vitesses et des températures sont également donnés et comparés aux solutions obtenues en supposant les propriétés physiques constantes.

Zusammenfassung—Es wird das stabile laminare Filmsieden bei freier Konvektion an einer isothermen senkrechten Wand oder an horizontalen Zylindern, die von gesättigter Flüssigkeit umgeben sind, untersucht. Hierzu werden die Methoden der Grenzschichttheorie angewendet und die Grenzschichtgleichungen in gewöhnliche Differentialgleichungen umgewandelt mit Hilfe einer Transformation, die ähnlich der für freie Konvektion und Kondensation ist. Die Gleichungen werden für kompressible Flüssigkeit mit veränderlicher spezifischer Wärme gelöst. Numerische Ergebnisse werden für Wasser in der Nähe des kritischen Punktes bei 193 und 214 bar mitgeteilt und bei Temperaturdifferenzen zwischen Wand und Flüssigkeit von 139, 278 und 555 grd. Ferner werden die Ergebnisse für den Wärmeübergang, die Geschwindigkeitsverteilung und die Temperaturverteilung angegeben und diese mit den Lösungen für konstante Stoffwerte verglichen.

Аннотация—Даётся анализ устойчивого ламинарного плёночного кипения в условиях свободной конвекции на изотермических вертикальных пластинах и горизонтальных цилиндрах, окруженных насыщенной жидкостью. Используется математический аппарат теории пограничного слоя, а уравнения пограничного сдоя сводятся к обычным дифференциальным уравнениям путём преобразований, аналогичных преобразованиям, применяемым в задачах свободной конвекции и конденсации. Уравнения решаются для сжимаемого потока с переменной удельной теплоёмкостью. Приводятся численные результаты для около критического состояния воды при давлениях, равных 2800 и 3100 фунт/кв. дюйм. и разностях температур между стенкой и жидкостью в 250, 500 и 1000°F. Приведены также результаты по теплообмену, распределению скоростей и температур в сравнении с решениями, полученными в предположении постоянства характеристик.

* Instructor, School of Mechanical Engineering. Purdue University.
† Professor of Mechanical Engineering. Purdue University, Lafayette, Indiana.

NOMENCLATURE

a, b, c, d = dimensionless constants;
c_1 = dimensional constant, $\left[\frac{g(\rho_L - \rho_{sat})\rho_{sat}}{4\mu^2 g_0^2}\right]^{1/4}, \frac{1}{ft^{3/4}}$;
c_2 = dimensionless constant, $\left[\frac{r^3 g(\rho_L - \rho_{sat})\rho_{sat}}{\mu^2 g_0^2}\right]^{1/4}$;
c_p = constant pressure specific heat (B.t.u./lb °F);*
f = function of β defined by equation (27);
g, $\mathbf{g}$ = acceleration or acceleration vector due to gravity, $4{\cdot}17 \times 10^8$ft/hr^2;
g_0 = dimensional constant, $4{\cdot}17 \times 10^8$ftlb/Lb hr^2;
$\mathbf{G}$ = body force per unit volume (Lb/ft^3);*
$\hbar$ = function of β defined by equation (27);
h_{fg} = enthalpy of evaporation (B.t.u./lb);
h = local convection heat transfer coefficient (B.t.u./ft^2 hr °F);
k = thermal conductivity (B.t.u./ft hr °F);
L = length of vertical plate (ft);
$N_{Nu,\lambda}$ = Nusselt number based on length λ;
N_{Pr} = Prandtl number
p = function of ξ, dimensionless;
P = pressure (Lb/ft^2);
q = local heat transfer rate (B.t.u./hr ft^2);
q''' = heat generation per unit volume (B.t.u./ft^{3}hr);
Q = total heat transferred (B.t.u./hr);
r = cylinder radius (ft);
T = temperature (°F);
T_{sat} = saturation temperature (°F);
T_w = wall temperature (°F);
t = dimensionless temperature defined by equation (27);
u = velocity component in the x-direction (ft/hr);
v = velocity component in the y-direction (ft/hr);
$\mathbf{V}$ = velocity vector (ft/hr);
x = co-ordinate along surface (ft);
y = co-ordinate normal to surface (ft);
β = angular co-ordinate (rad);
δ = thickness of vapor film (ft);
ζ = dimensionless function defined by equation (16);
η = dimensionless independent variable $c_1 y/x^{1/4}$.
θ = dimensionless temperature, $(T - T_{sat})/(T_w - T_{sat})$;
Θ = $(T_w - T_{sat})$ (°F);
μ = viscosity (Lb hr/ft^2);
ξ = dimensionless independent variable defined by equation (27):
ρ = vapor density (lb/ft^3);
ρ_L = liquid density (lb/ft^3);
ρ_{sat} = saturated vapor density (lb/ft^3):
τ = time (hr);
ϕ = dimensionless independent variable, $c_2 y/r$;
ψ = stream function (ft^2/hr);
Ψ = dimensionless stream function defined by equation (24);
∇ = vector operator used for, say, the gradient of a scalar;
∇^2 = Laplace operator.

Subscripts

cp = constant properties;
vp = vertical plate;
c = horizontal cylinder;
x = x-direction.

* The abbreviation for the pound mass is lb, and for pound force is Lb throughout the paper.

INTRODUCTION

ALTHOUGH the first observation of the phenomenon of film boiling was made in 1746, an analytical treatment was not suggested until almost two centuries later. In 1941, Colburn [1] suggested that Nusselt's [2] theory on laminar film condensation could be modified for the case of laminar film boiling. In 1950, Bromley [3] presented a model for the case of stable laminar film boiling on the outside of a horizontal cylinder. By assuming an isothermal wall, a saturated liquid, pure conduction heat transfer across the film and by neglecting inertia in the vapor layer, he derived an expression for the convection coefficient. The free convection heat

transfer was expressed in terms of a Nusselt number as

$$N_{\mathrm{Nu},D} = c\left[\frac{g(\rho_L - \rho)\,\rho D^3 h_{fg}}{k\mu g_0 \Theta}\right]^{1/4} \quad (1)$$

where the properties were evaluated at an average temperature. The constant c depended upon the boundary conditions at the interface. For zero velocity at the interface c was 0·512, for zero shear stress at the interface c was 0·724. This latter condition is the boundary condition considered in the case of laminar film condensation, the former is usually associated with film boiling. This gives the extremes between which the actual case lies in film boiling and also indicates how liquid movement can influence the results.

In 1952, Bromley [4] modified the theory to take into account the superheating of the vapor film. Cess [5] arrived at an expression similar to equation (1) by assuming a temperature profile in the vapor layer and by considering the effect of the liquid–vapor interfacial shear stress. Chang [6] has presented a wave theory for film boiling. In 1958, Sparrow and Gregg [7] proposed an exact analysis of laminar film condensation with constant properties which is similar to that used in the present paper for laminar film boiling. Both investigations were performed independently of each other.

In the theory presented to date for stable, laminar film boiling on isothermal surfaces, no attempt has been made to consider variable properties. In this paper the writers will show how the severe variations of specific heat and density with temperature near the critical pressure can be exactly considered by treating film boiling with boundary-layer theory. The complete boundary-layer equations will be solved, and the results obtained will be compared with the approximate theories available. Radiation will not be considered in order to investigate only the variable property effects on convection.

FUNDAMENTAL EQUATIONS

The fundamental equations which express the laws of conservation for mass, momentum and energy for stable, laminar, free convection, film boiling were written as follows:

$$\frac{\partial \rho}{\partial \tau} + \nabla(\rho \mathbf{V}) = 0 \quad (2)$$

$$\frac{\rho}{g_0}\frac{\mathrm{d}\mathbf{V}}{\mathrm{d}\tau} = \mu\nabla^2\mathbf{V} - \nabla P + \mathbf{G} + \frac{\mu}{3}\nabla(\nabla \cdot \mathbf{V}) \quad (3)$$

$$\rho c_p \frac{\mathrm{d}T}{\mathrm{d}\tau} = k\nabla^2 T + q''' \quad (4)$$

Equations (2) through (4) were valid for compressible flow with variable specific heat. Viscosity and thermal conductivity were assumed constant since their variation was one-half order of magnitude, or more, less than the variation in density and specific heat for the situations considered in this paper.

In order to solve these equations, some additional assumptions were necessary. Only steady, two-dimensional boundary-layer flow was considered as shown in Fig. 1A; thus equations (2) through (4) became

$$\frac{\partial(\rho u)}{\partial x} + \frac{\partial(\rho v)}{\partial y} = 0 \quad (5)$$

$$\frac{\rho}{g_0}\left(u\frac{\partial u}{\partial x} + v\frac{\partial u}{\partial y}\right) = u\frac{\partial^2 u}{\partial y^2} - [\nabla P]_x + [\mathbf{G}]_x \quad (6)$$

$$\rho c_p\left(u\frac{\partial T}{\partial x} + v\frac{\partial T}{\partial y}\right) = k\frac{\partial^2 T}{\partial y^2} \quad (7)$$

where the heat generation per unit volume was assumed to be zero. Schlichting [8] shows that these equations are also valid for the case of a cylinder, as shown in Fig. 1B, if the boundary layer thickness is small compared to the cylinder radius.

An isothermal wall was assumed as well as a saturated liquid which was everywhere at rest; thus, the boundary conditions for the above equations became

$$\left.\begin{aligned} u = v = 0,\ T = T_w \qquad & y = 0 \\ u = 0,\ T = T_{\mathrm{sat}} \qquad & y = \delta \end{aligned}\right\} \quad (8)$$

An additional condition was required because the film thickness δ was not known *a priori*. This was obtained by noting that all the heat transferred by conduction at the liquid–vapor interface was used to vaporize liquid; that is

$$q = \rho_{\mathrm{sat}}\, h_{fg}\, v = -k\frac{\partial T}{\partial y} \qquad y = \delta \quad (9)$$

Equations (5) through (7) with conditions given by equations (8) and (9) are the simplified equations which were solved for the case of film boiling from a vertical plate and a horizontal cylinder.

The first step in the solution of equations (5) through (9) was the introduction of a stream function; that is

$$\rho u = \rho_{sat} \frac{\partial \psi}{\partial y}, \quad \rho v = - \rho_{sat} \frac{\partial \psi}{\partial x} \tag{10}$$

This substitution eliminated equation (5) and equations (6) and (7) became

$$\left.\begin{aligned} &\frac{\partial \psi}{\partial y}\frac{\partial^2 \psi}{\partial x \partial y} - \frac{\partial \psi}{\partial x}\frac{\partial^2 \psi}{\partial y^2} - \frac{\rho g_0}{\rho^2_{sat}}\{[\nabla P]_x - [\mathbf{G}]_x\} \\ &\quad - \frac{\mu g_0}{\rho_{sat}}\frac{\partial^3 \psi}{\partial y^3} \\ &\quad = \frac{1}{\rho}\frac{\partial \rho}{\partial x}\left(\frac{\partial \psi}{\partial y}\right)^2 - \frac{1}{\rho}\frac{\partial \psi}{\partial x}\frac{\partial \psi}{\partial y}\frac{\partial \rho}{\partial y} \\ &\quad - \frac{2\mu g_0}{\rho\,\rho_{sat}}\frac{\partial \rho}{\partial y}\frac{\partial^2 \psi}{\partial y^2} \\ &\quad - \frac{\mu g_0}{\rho \rho_{sat}}\frac{\partial \psi}{\partial y}\left\{\frac{\partial^2 \rho}{\partial y^2} - \frac{2}{\rho}\left(\frac{\partial \rho}{\partial y}\right)^2\right\} \end{aligned}\right\} \tag{11}$$

and

$$\frac{\partial \psi}{\partial y}\frac{\partial T}{\partial x} - \frac{\partial \psi}{\partial x}\frac{\partial T}{\partial y} = \frac{k}{\rho_{sat} c_p}\frac{\partial^2 T}{\partial y^2} \tag{12}$$

The boundary conditions in equation (8) became

$$\left.\begin{aligned} &\frac{\partial \psi}{\partial y} = \frac{\partial \psi}{\partial x} = 0, \; T = T_w && y = 0 \\ &\frac{\partial \psi}{\partial y} = 0, \; T = T_{sat}, \; \frac{\partial T}{\partial y} = \frac{h_{fg}}{k}\rho_{sat}\frac{\partial \psi}{\partial x}, && y = \delta \end{aligned}\right\} \tag{13}$$

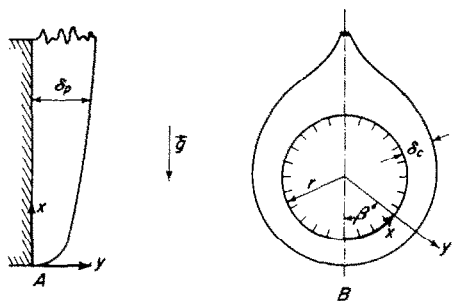

FIG. 1. Physical model and co-ordinate system for: A, plane wall and B, horizontal cylinder

It remained to reduce these to ordinary differential equations to facilitate solution.

REDUCTION OF EQUATIONS

Equations (11), (12) and (13) were simplified by expressing the pressure gradient and body force in terms of specific weights and by introducing a similarity transformation which reduced the partial to ordinary differential equations. These steps will now be described.

Plane vertical wall

The pressure gradient in the x-direction was the hydrostatic pressure gradient

$$[\nabla P]_x = - \frac{g}{g_0}\rho_L \tag{14}$$

and body force in the x-direction was the gravity force on the vapor,

$$[\mathbf{G}]_x = - \frac{g}{g_0}\rho \tag{15}$$

The sum of the pressure gradient and body force

$$\frac{g(\rho_L - \rho)}{g_0}$$

gave the bouyant force. By introducing a similarity transformation, equations (11) and (12) were made ordinary. To this end

$$\left.\begin{aligned} \eta &= c_1 \frac{y}{x^{1/4}} \\ \psi &= 4\frac{\mu g_0}{\rho_{sat}} c_1 x^{3/4}\zeta(\eta) \end{aligned}\right\} \tag{16}$$

where

$$c_1 = \left[\frac{g(\rho_L - \rho_{sat})\,\rho_{sat}}{4\,\mu^2 g_0^2}\right]^{1/4} \tag{17}$$

were introduced where η was a new independent variable. Also, at a given pressure, density was a function only of temperature thus

$$\frac{\partial \rho}{\partial x} = \frac{d\rho}{dT}\frac{\partial T}{\partial x}, \quad \frac{\partial \rho}{\partial y} = \frac{d\rho}{dT}\frac{\partial T}{\partial y} \tag{18}$$

Introducing the above in equations (11) and (12) there resulted

$$\left.\begin{aligned}\zeta''' + 3\zeta\zeta'' - 2(\zeta')^2 + \frac{(\rho_L - \rho)\,\rho}{(\rho_L - \rho_{sat})\,\rho_{sat}} = \\ = \frac{1}{\rho}\frac{d\rho}{d\theta}\theta'[3\zeta\zeta' + 2\zeta''] + \\ + \frac{1}{\rho}\zeta'(\theta')^2\left[\frac{d^2\rho}{d\theta^2} - \frac{2}{\rho}\left(\frac{d\rho}{d\theta}\right)^2\right] + \frac{1}{\rho}\frac{d\rho}{d\theta}\zeta'\theta''\end{aligned}\right\} \quad (19)$$

$$\theta'' + 3\frac{\mu g_0}{k}c_p\,\zeta\theta' = 0 \quad (20)$$

where the primes on ζ and θ represent differentiation with respect to η. The boundary conditions on this set of equations were obtained from equations (9) and (13) as:

$$\left.\begin{aligned}\zeta = \zeta' = 0,\ \theta = 1 \qquad \eta = 0 \\ \zeta' = 0,\ \theta = 0,\ \theta' = -3\frac{\mu g_0}{k}\frac{h_{fg}}{\Theta}\zeta \quad \eta = \eta_\delta\end{aligned}\right\} \quad (21)$$

The simultaneous solution of equations (19) and (20) with the boundary conditions above, completely described the temperature and velocity distributions and also the heat transfer for stable, laminar free convection film boiling where radiation is not important.

It should be noted that the results for the vertical plate can also be applied to the vertical cylinder if δ/r is less than 0·03. This should introduce an error of about 1 per cent in the film thickness according to Greenburg [9].

Horizontal cylinder

The pressure gradient in the x-direction was the hydrostatic pressure gradient again

$$[\nabla P]_x = -\frac{g}{g_0}\rho_L \sin\frac{x}{r} \quad (22)$$

and the body force in the x-direction

$$[G]_x = -\frac{g}{g_0}\rho\sin\frac{x}{r} \quad (23)$$

was the gravity force on the vapor.

The first step in reducing equations (11) and (12) to ordinary differential equations was to introduce the following

$$\left.\begin{aligned}\beta &= \frac{x}{r} \\ \phi &= c_2\frac{y}{r} \\ \Psi &= \frac{\psi\ \rho_{sat}}{c_2\,\mu g_0} \\ c_2 &= \left[\frac{r^3 g(\rho_L - \rho_{sat})\,\rho_{sat}}{\mu^2 g_0^2}\right]^{1/4}\end{aligned}\right\} \quad (24)$$

In this way, equations (11) and (12) became

$$\left.\begin{aligned}\frac{\partial\Psi}{\partial\phi}\frac{\partial^2\Psi}{\partial\beta\partial\phi} - \frac{\partial\Psi}{\partial\beta}\frac{\partial^2\Psi}{\partial\phi^2} - \\ \frac{(\rho_L - \rho)\,\rho}{(\rho_L - \rho_{sat})\,\rho_{sat}}\sin\beta - \frac{\partial^3\Psi}{\partial\phi^3} \\ = \frac{1}{\rho}\left(\frac{\partial\Psi}{\partial\phi}\right)^2\frac{\partial\rho}{\partial\beta} - \frac{1}{\rho}\frac{\partial\Psi}{\partial\phi}\frac{\partial\Psi}{\partial\beta}\frac{\partial\rho}{\partial\phi} \\ - \frac{2}{\rho}\frac{\partial\rho}{\partial\phi}\frac{\partial^2\Psi}{\partial\phi^2} \\ - \frac{1}{\rho}\frac{\partial\Psi}{\partial\phi}\left[\frac{\partial^2\rho}{\partial\phi^2} - \frac{2}{\rho}\left(\frac{\partial\rho}{\partial\phi}\right)^2\right]\end{aligned}\right\} \quad (25)$$

$$\frac{\partial\Psi}{\partial\phi}\frac{\partial\theta}{\partial\beta} - \frac{\partial\Psi}{\partial\beta}\frac{\partial\theta}{\partial\phi} = \frac{k}{\mu g_0 c_p}\frac{\partial^2\theta}{\partial\phi^2} \quad (26)$$

To simplify these, the following substitutions were used

$$\left.\begin{aligned}\xi &= \phi\,\hbar(\beta) \\ \Psi(\beta,\phi) &= p(\xi)\,f(\beta) \\ \theta(\beta,\phi) &= t(\xi)\end{aligned}\right\} \quad (27)$$

and then equations (25) and (26) became

$$\left.\begin{aligned}p'''\{f\hbar^3\} + pp''\{ff'\hbar^2\} - (p')^2\{f^2\hbar'\hbar + \\ + \hbar^2 f'f\} + \frac{(\rho_L - \rho)\,\rho}{(\rho_L - \rho_{sat})\,\rho_{sat}}\sin\beta = \\ = \frac{1}{\rho}\frac{\partial\rho}{\rho\xi}\{\hbar^2 f'fpp' + 2\hbar^3 fp''\} + \\ + \left[\frac{\partial^2\rho}{\partial\xi^2} - \frac{2}{\rho}\left(\frac{\partial\rho}{\partial\xi}\right)^2\right]\frac{1}{\rho}\hbar^3 fp'\end{aligned}\right\} \quad (28)$$

and

$$t''\hbar + \frac{\mu g_0}{k}c_p\,pt'f' = 0 \quad (29)$$

where primes on t and p represent differentiation with respect to ξ and primes on f and h represent differentiation with respect to β. Now, when

$$\left.\begin{aligned} f'(\beta) &= a\hbar(\beta) \\ f^2(\beta)\hbar(\beta)\hbar'(\beta) &= b\sin\beta \\ f(\beta)\hbar^2(\beta)f'(\beta) &= c\sin\beta \\ f(\beta)\hbar^3(\beta) &= d\sin\beta \end{aligned}\right\} \quad (30)$$

equations (28) and (29) could be written as

$$\left.\begin{aligned} &p'''d + pp''c - (p')^2\{b + c\} + \\ &+ \frac{(\rho_L - \rho)\,\rho}{(\rho_L - \rho_{\text{sat}})\,\rho_{\text{sat}}} = \\ &= \frac{1}{\rho}\frac{\partial\rho}{\partial\xi}\{cpp' + 2p''d\} + \\ &+ \frac{1}{\rho}p'd\left[\frac{\partial^2\rho}{\partial\xi^2} - \frac{2}{\rho}\left(\frac{\partial\rho}{\partial\xi}\right)^2\right] \end{aligned}\right\} \quad (31)$$

$$t'' + a\frac{\mu g_0}{k}c_p pt' = 0 \quad (32)$$

Fortunately, equations (30) were solved by Hermann [10] who gives graphs of $\hbar$ and $f\hbar$ vs. β, and values for the constants as follows: $a = 3$, $b = -1$, $c = 3$ and $d = 1$.

Finally, using values for the constants a through d, equations (31) and (32) became

$$\left.\begin{aligned} &p''' + 3pp'' - 2(p')^2 + \frac{(\rho_L - \rho)\,\rho}{(\rho_L - \rho_{\text{sat}})\,\rho_{\text{sat}}} = \\ &= \frac{1}{\rho}\frac{\mathrm{d}\rho}{\mathrm{d}t}t'[3pp' + 2p''] + \frac{1}{\rho}p'\frac{\mathrm{d}\rho}{\mathrm{d}t}t'' + \\ &+ \frac{1}{\rho}p'(t')^2\left[\frac{\mathrm{d}^2\rho}{\mathrm{d}t^2} - \frac{2}{\rho}\left(\frac{d\rho}{dt}\right)^2\right] \end{aligned}\right\} \quad (33)$$

$$t'' + 3\frac{\mu g_0}{k}c_p pt' = 0 \quad (34)$$

The boundary conditions on equations (33) and (34) were

$$\left.\begin{aligned} &p = p' = 0,\ t = 1 && \xi = 0 \\ &p' = 0,\ t = 0,\ t' = -3\frac{\mu g_0}{k}\frac{h_{fg}}{\Theta}p && \xi = \xi_\delta \end{aligned}\right\} \quad (35)$$

Thus it is seen that these are the same differential equations and boundary conditions which were set up for the case of the flat plate.

Relation between heat transfer on cylinder and on plate

Since the reduced differential equations were the same for the plate and cylinder, it was expected that the heat transfer for each was related.

For the vertical plate the local wall heat transfer could be expressed as

$$q_w = -k\left(\frac{\partial T}{\partial y}\right)_w = -k\,\Theta\,c_1 x^{-1/4}\left(\frac{\mathrm{d}\theta}{\mathrm{d}\eta}\right)_w = \\ = -h_{vp}\,\Theta \quad (36)$$

and an average heat-transfer coefficient was found by integrating the local coefficient over the entire plate. Thus

$$(h_{vp})_{\text{avg}} = \frac{1}{\Theta L}\int_0^L k\,\Theta\,c_1\left(\frac{\mathrm{d}\theta}{\mathrm{d}\eta}\right)_w x^{-1/4}\,\mathrm{d}x = \\ = k\,c_1\left(\frac{\mathrm{d}\theta}{\mathrm{d}\eta}\right)_w\frac{4}{3L^{1/4}} \quad (37)$$

The heat transfer may also be expressed in terms of an average Nusselt number as

$$N_{\text{Nu},L} = \frac{4}{3}L^{3/4}c_1\left(\frac{\mathrm{d}\theta}{\mathrm{d}\eta}\right)_w \quad (38)$$

We now consider the horizontal cylinder. In the case of the horizontal cylinder the wall heat flux could be expressed as

$$q_w = -k\left(\frac{\partial T}{\partial y}\right)_w = -k\Theta\frac{c_2}{r}\left(\frac{\partial\theta}{\partial\phi}\right)_w \\ -k\,\Theta\frac{c_2}{r}\hbar(\beta)\left(\frac{\mathrm{d}t}{\mathrm{d}\xi}\right)_w = -h_c\,\Theta \quad (39)$$

and an average heat-transfer coefficient was found by integrating the local coefficient over the entire cylinder. Thus

$$(h_c)_{\text{avg}} = \frac{1}{\Theta\pi}\int_0^\pi k\Theta\frac{c_2}{r}\left(\frac{\mathrm{d}t}{\mathrm{d}\xi}\right)_w\hbar(\beta)\,\mathrm{d}\beta \\ = \frac{(1{\cdot}91)k\,c_2}{\pi r}\left(\frac{\mathrm{d}t}{\mathrm{d}\xi}\right)_w \quad (40)$$

which followed from Hermann's [10] graphical integration where

$$\int_0^\pi\hbar(\beta)\,\mathrm{d}\beta = 1{\cdot}91 \quad (41)$$

The heat transfer was expressed in terms of an average Nusselt number as

$$[N_{\mathrm{Nu},D} = 1{\cdot}025\, c_2 \left(\frac{\mathrm{d}t}{\mathrm{d}\xi}\right)_w \qquad (42)$$

The similarity between equations (38) and (42) is now apparent.

For a given fluid surrounding a plate or cylinder at the same pressure and with the same wall to fluid temperature difference it followed that

$$\left(\frac{\mathrm{d}\theta}{\mathrm{d}\eta}\right)_w = \left(\frac{\mathrm{d}t}{\mathrm{d}\xi}\right)_w \qquad (43)$$

Therefore, for identical characteristic lengths

$$\frac{(h_c)_{\mathrm{avg}}}{(h_{vp})_{\mathrm{avg}}} = 0{\cdot}77 \qquad (44)$$

and

$$\frac{Q_c}{Q_{vp}} = 2{\cdot}42 \qquad (45)$$

Thus, once the vertical flat plate problem was solved, heat transfer results were transferred directly to the horizontal cylinder or vice versa.

SOLUTION OF EQUATIONS

The reduced differential equations for the plate and cylinder, equations (19) and (20) were identical. They were solved numerically by the Runge–Kutta [11] method on a Datatron 204 digital computer for the cases where: (a) properties were constant, (b) specific heat and bouyant force were variable, and (c) specific heat and density were variable. Equations for the two former cases were easily derived from equations (19) and (20). The calculations were performed for water at two different pressure levels, 2800 and 3100 lb/in^2. The critical pressure for water is thought to be slightly above 3200 lb/in^2.

The increments in the independent variable used in the Runge–Kutta method were 0·01 and 0·05 at the low- and high-pressure levels, respectively. It was observed that decreasing the interval from 0·1 to 0·01 changed the results for θ' at η equal to zero by less than 5 per cent.

Initial conditions on velocity and temperature and their derivatives with respect to η were required for the computer. Since the boundary conditions in this problem were mixed, that is, three were given at η equal to zero and three at η_δ, as indicated in equation (21), it was necessary to estimate ζ'' and θ' initially. The initial estimate was then refined until ζ' and θ went to zero at η equal to η_δ and at the same time equation (21) was satisfied. It was considered adequate to satisfy the last of equations (21) within ± 5 per cent; since, this introduced at most an error of from 1 to 2 per cent in θ' at η equal to zero.

Variable properties and their first and second derivatives with respect to temperature were tabulated and stored in the computer for each 0·01 interval of the dimensionless temperature excess. A linear interpolation was used for values between those stored.

Saturation and density data were obtained from Keenan and Keyes [12]. For densities at temperatures higher than the tabulated values, the data from Keenan and Keyes was faired into the ideal-gas equation of state. This would introduce at most an error of about 3 per cent excluding the inaccuracy of values in the table to which values were faired. Values for $\mathrm{d}\rho/\mathrm{d}\theta$ and $\mathrm{d}^2\rho/\mathrm{d}\theta^2$ were obtained numerically from a plot of ρ vs. θ. Values of $\mathrm{d}\rho/\mathrm{d}\theta$ and $\mathrm{d}^2\rho/\mathrm{d}\theta^2$ at $\theta = 0{\cdot}00$ and $\theta = 1{\cdot}00$ were extrapolated. Numerical evaluation such as this was not highly accurate, but gave a good approximation. The specific heat was also taken from Keenan and Keyes [12], and data for temperatures beyond those given in the reference were extrapolated according to the curves given in the reference. The viscosity and thermal conductivity were taken from Dsrjinskogo [13], and data for temperatures beyond those listed in the tables were extrapolated according to the curves given in the reference. At all times, interpolations between given points were taken linearly. In those cases where properties were considered constant they were evaluated at the arithmetic mean wall and saturation temperature.

RESULTS

The effects of considering variable properties at pressures approaching the critical pressure were illustrated by the results obtained from the solution of equations (19) and (20) for the three specified cases. The significant results are presented in Table 1. Table 2 presents a comparison of results obtained considering: (1) all

Table 1. Significant results

		Compressible			Incompressible			All properties constant				
P (lb/in^2)	Θ (°F)	η_δ	$\zeta'_{\max}$	$\left(\frac{d\theta}{d\eta}\right)_w$	η_δ	$\zeta'_{\max}$	$\left(\frac{d\theta}{d\eta}\right)_w$	$\frac{c_p\Theta}{h_{fg}}$	N_{Pr}	η_δ	$\zeta'_{\max}$	$\left(\frac{d\theta}{d\eta}\right)_w$
2800	250	1·39	0·17	0·76	0·96	0·25	1·14	0·92	1·26	1·27	0·181	0·88
	500	1·64	0·19	0·67	1·04	0·35	1·09	1·32	1·0	1·43	0·233	0·79
	1000	1·84	0·21	0·62	1·14	0·47	1·04	2·3	0·90	1·60	0·285	0·73
3100	250	2·35	0·093	0·48				1·8	1·45	1·37	0·214	0·84
	500	2·83	0·103	0·41				2·3	1·0	1·56	0·271	0·75
	1000	3·15	0·113	0·39				3·8	0·88	1·69	0·302	0·71

properties constant; (2) variable specific heat with density variations considered only in the evaluation of the bouyant force, and (3) compressible flow with variable specific heat. The comparisons of heat transfer, maximum velocity and film thickness were made according to the following. Since

$$q = -k\frac{\partial T}{\partial y} = -k\Theta c_1 x^{-1/4}\frac{d\theta}{d\eta} \tag{46}$$

for the same wall to liquid temperature difference and the same value of x,

$$\frac{q}{q_{cp}} = \frac{\{c_1(d\theta/d\eta)\}}{\{c(d\theta/d\eta)\}_{cp}} \tag{47}$$

was used to compare the heat transfer as calculated by constant property and variable property analyses. Also since

$$u = 4\frac{\mu g_0}{\rho_{sat}} c_1^2 \zeta' \tag{48}$$

and

$$\eta_\delta = c_1\frac{y}{x^{1/4}} \tag{49}$$

for the same wall-to-liquid temperature difference and the same value of x,

$$\frac{u_{\max}}{(u_{\max})_{cp}} = \frac{\rho_{cp}}{\rho_{sat}}\left(\frac{c_1}{c_{cp}}\right)^2\frac{\zeta'_{\max}}{(\zeta'_{\max})_{cp}} \tag{50}$$

and

$$\frac{\delta}{\delta_{cp}} = \frac{c_{cp}}{c_1}\frac{\eta_\delta}{(\eta_\delta)_{cp}} \tag{51}$$

were used to compare the maximum velocity and film thickness, respectively, as calculated by the three methods.

It was of interest to note that if at a given pressure $u/u_{\max}$ was plotted against y/δ, the data fell very close to a single curve no matter what the wall temperature, as shown in Fig. 2. If data for different pressures were compared in this matter, the position of the maximum velocity was seen to vary as shown in Fig. 3. For constant properties the maximum velocity occurs at $y/\delta = 1/2$. The shifting of the velocity maximum was not easily explained. However, if inertia terms were neglected in equation (6), $(\rho_L - \rho)/\rho$ was assumed to decrease linearly from the wall to the liquid–vapor interface, and other properties were considered constant, it was seen that the velocity maximum should be shifted in the direction indicated.

Table 2. A comparison of results

		Compressible			Incompressible	
P (lb/in^2)	Θ (°F)	$\frac{q}{q_{cp}}$	$\frac{u_{\max}}{u_{(\max cp)}}$	$\frac{\delta}{\delta_{cp}}$	$\frac{q}{q_{cp}}$	$\frac{\delta}{\delta_{cp}}$
2800	250	0·96	0·61	0·98	1·66	0·66
	500	0·98	0·47	0·99	1·6	0·62
	1000	1·04	0·37	0·94	1·63	0·59
3100	250	0·65	0·23	1·55		
	500	0·64	0·17	1·57		
	1000	0·63	0·145	1·53		

As seen in Table 2, the effect of considering compressible flow was to decrease the maximum

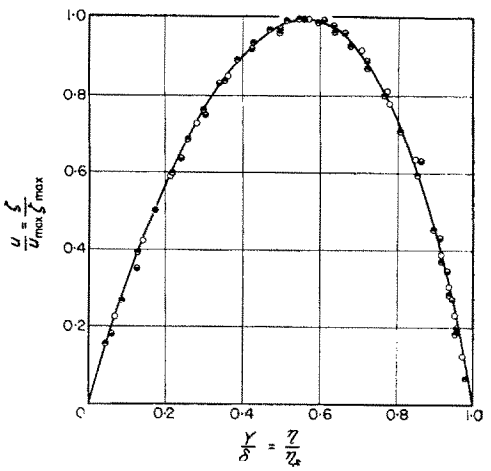

FIG. 2. Dimensionless velocity distribution for water vapor, $P = 3100$ lb/in²

- ◓ $\Theta = 250°F$
- ○ $\Theta = 500°F$
- ◒ $\Theta = 1000°F$

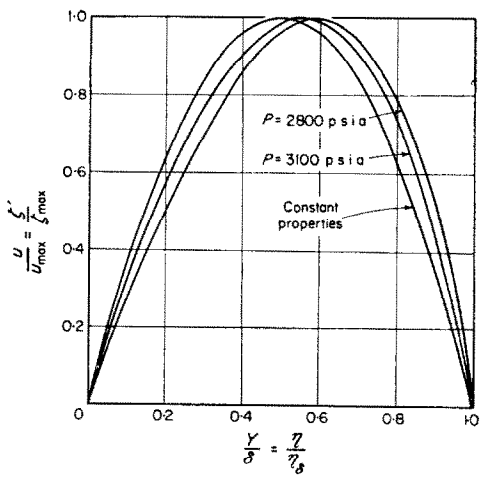

FIG. 3. Comparison of dimensionless velocity distributions

velocity in the film. This would tend to offset the increase in shear stress at the liquid–vapor interface caused by the shifting of the maximum velocity.

The temperature profiles at three different wall-to-liquid temperature differences at 2800 and 3100 lb/in² are shown in Figs. 4 and 5, respectively. Note that if the compressible-flow temperature profiles for the same value of $c_p\Theta/h_{fg}$ are plotted against y/δ, the curves are identical as shown in Fig. 6.

The effect on the temperature profile of considering a variable specific heat and bouyant force but otherwise incompressible flow is shown in Fig. 7. The profiles for only one wall-to-liquid temperature difference are shown, the effect being the same for all other cases investigated.

The effect of considering the vapor as incompressible while taking into account the variation

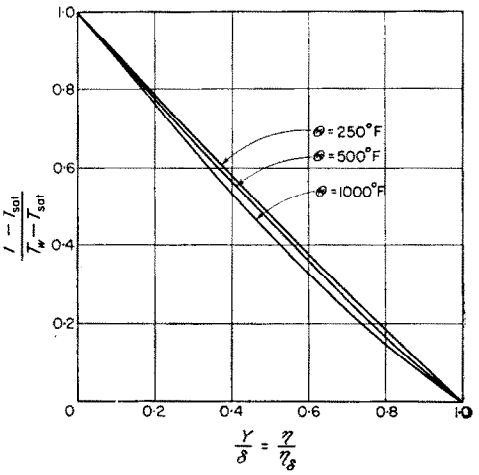

FIG. 4. Dimensionless temperature distribution in the vapor layer considering variable properties, water at 2800 lb/in².

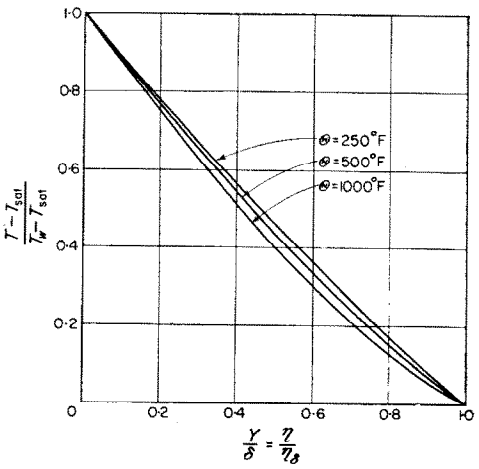

FIG. 5. Dimensionless temperature distribution in the vapor layer considering variable properties, water at 3100 lb/in².

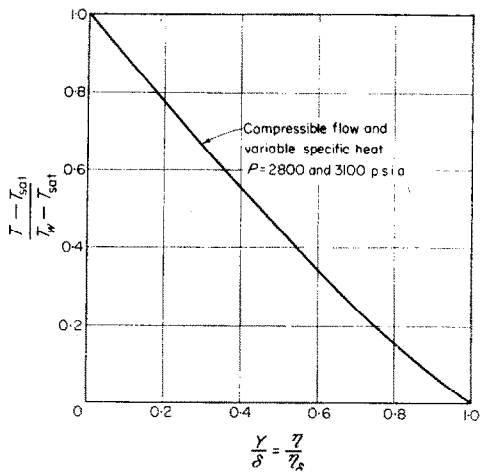

FIG. 6. Comparison of temperature distributions for $cp\Theta/h_{fg} = 2{\cdot}3$

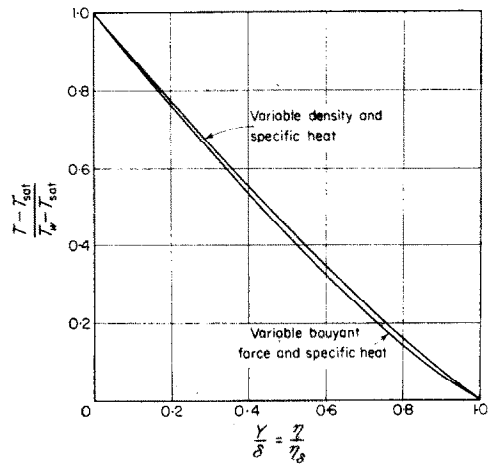

FIG. 7. The effect of an incompressible fluid with variable bouyant force and specific heat on temperature distribution, water at 2800 lb/in², $\Theta = 1000°F$

of specific heat and bouyant force was to increase the heat transfer by about 60 per cent at 2800 lb/in², as shown in Table 2. When compressible flow as well was considered, the variable-property analysis gave no significantly different results than the constant-property analysis at 2800 lb/in², provided the properties were evaluated at the mean temperature.

At 3100 lb/in² the decrease in film velocity due to considering compressible flow increased the film thickness appreciably. The effect was to decrease the heat transfer compared to that expected with a constant-property analysis.

CONCLUSION

The results of this investigation showed that the heat transfer as calculated by the constant-property method did not always agree with the heat transfer as calculated by the variable-property methods. For water at 2800 lb/in² the consideration of compressible flow and variable specific heat did not appreciably change the heat transfer from that calculated by assuming constant properties, provided the constant properties were evaluated at the arithmetic mean film temperature. At 3100 lb/in², however, the heat transfer as calculated by assuming constant properties was from 54 to 59 per cent greater than the heat transfer as calculated by considering compressible flow and variable specific heat.

The method of considering variable specific heat while density variations were used only in the evaluation of the bouyant force was not valid. The variable specific heat tends to increase the wall heat transfer; the variable density thickens the vapor layer and thus tends to decrease the heat transfer.

At 2800 and 3100 lb/in² radiation plays a more important role in film boiling than does the consideration of variable properties.

Actually, 3100 lb/in² is still very far from the critical pressure. It is felt that as the critical pressure is approached even more closely, the role that variable properties play in film-boiling heat transfer will become increasingly important. The work required near the critical pressure can not be completed, however, until more accurate property values in this region are available.

ACKNOWLEDGEMENT

The writers wish to thank Argonne National Laboratory, and ultimately the Atomic Energy Commission for making this work possible through Argonne National Laboratory Subcontract 31-109-38-704. We particularly wish to thank Dr. P. Lottes of Argonne National Laboratory for his advice and encouragement throughout this work.

REFERENCES

1. J. W. WESTWATER, Boiling of Liquids in *Advances in Chemical Engineering* (Edited by T. B. DREW and J. W. HOOPES, JR.), Vol. II. Academic Press, New York (1958).

2. W. NUSSELT, *Z. Ver. dtsch. Ing.* **60**, 541 and 569 (1916).
3. L. A. BROMLEY, *Chem. Engng. Progr.* **46**, 221 (1950).
4. L. A. BROMLEY, *Industr. Engng. Chem.* **44**, 2966 (1952).
5. R. D. CESS, A personal communication concerning unpublished work.
6. V. P. CHANG, *J. Heat Transfer* 1 (1959).
7. E. M. SPARROW and J. L. GREGG, *J. Heat Transfer* 13 (1959).
8. H. SCHLICHTING, *Boundary Layer Theory* (Translated by J. KESTIN) McGraw-Hill, New York (1955).
9. A. B. GREENBURG, *Mechanics of Film Flow on a Vertical Surface*. Ph.D. Thesis, Purdue University (1956).
10. R. HERMANN, *Heat Transfer by Free Convection from Horizontal Cylinders in Diatomic Gases*. NACA TM 1366.
11. F. B. HILDEBRAND, *Introduction to Numerical Analysis*. McGraw-Hill, New York (1956).
12. J. H. KEENAN and F. G. KEYES, *Thermodynamic Properties of Steam* (1st Ed.). John Wiley, New York (1951).
13. F. E. DSRJINSKOGO, *Tables of Thermodynamic Properties of Water and Water Vapor Based on Experimental Data*. Governmental Energetical Publishing House, Moscow (1952).